Optimization of Tumor Spheroid Preparation and Morphological Analysis for Drug Evaluation

Optimization of Tumor Spheroid Preparation and Morphological Analysis for Drug Evaluation

Jaehun Lee [a,b,1], Youngwon Kim [a,b,1], Ji Seok Lim [c,d], Hyo-Il Jung [a,e], Gastone Castellani [f], Filippo Piccinini [f,g], and Bong Seop Kwak [b,d*]

[a] Yonsei University, School of Mechanical Engineering, Seoul, Republic of Korea

[b] Dongguk University, College of Medicine, Goyangsi, Gyeonggi-do, Republic of Korea

[c] Yeungnam University, School of Mechanical Engineering, Gyeongsan-si, Gyeongsanbuk-do, Republic of Korea

[d] MediSphere Inc., Gyeongsan-si, Gyeongsanbuk-do, Republic of Korea

[e] The DABOM Inc., Seodaemun-gu, Seoul, Republic of Korea

[f] Department of Medical and Surgical Sciences (DIMEC), University of Bologna, Bologna, Italy

[g] IRCCS Istituto Romagnolo per lo Studio dei Tumori (IRST) "Dino Amadori", Meldola, Italy

*Corresponding author

E-mail address: bskwak82@gmail.com

Telephone number: +82-31-961-5803

Mobile-phone number: +82-10-4477-3865

[1] These authors contributed equally to this paper.

Keywords: Tumor spheroid, Droplet-based microfluidic system, Spheroid compaction, Necrotic core, AI-based morphological analysis

Abstract

Due to its similarity to *in vivo* conditions, tumor spheroids are actively used in research areas such as drug screening and cell-cell interactions. A significant number of samples is essential to obtain reliable results in drug screening, and a droplet-based microfluidics system capable of mass-producing spheroids can meet this demand. In this study, we investigated the optimal culture conditions, which allows to researchers provide guidelines for producing spheroids with the desired diameter and quantity. Mass-produced spheroids were employed to analyze compaction, which is crucial for evaluating the remission effects of drugs, as well as the formation of a necrotic core, which induces a bias in the analysis of drug response and viability. The time point at which compaction is completed and the diameter begins to increase was measured using spheroids with diameters of both >400μm and <400μm, and spheroids do not proliferate a linear growth trend. Spheroid with diameters ranging from 73 to 371μm were used to predict the formation of the necrotic core based on live cell counting, and a diameter of 315.3μm was mathematically calculated as the diameter where a necrotic core forms. Additionally, the use of artificial intelligence (AI) for high-throughput analysis is crucial for obtaining time-saving and reproducible data. We produced BT474 and MCF-7 spheroids with diameters of 100, 200, and 300μm and obtained morphological indicators from an AI-based program to compare the differences in heterogeneous breast tumor spheroids. Through this study, we optimized the diameter of spheroids and the initiation timing for drug screening and emphasized the importance of AI-based morphological analysis in high-throughput screening.

1. Introduction

Two major methods used in biology research and drug development are cell monolayer and spheroid (or organoid) [1]. Cell monolayer can have challenges in replicating *in-vivo* microenvironment because cells are positioned on a flat surface [2]. While, spheroids more accurately mimic the microenvironment of the human body, enabling a more realistic drug response because, within a spheroid, cells interact naturally in a three-dimensional space, promoting cell-cell interactions [3,4]. Many researchers recognize the significance of spheroids for studies involving cell-cell interactions [5], biological analysis [6], and drug responses [7, 8]. However, current techniques such as hanging drop plates [9], microcavity methods [10], and ultra-low adhesive surfaces [11] to produce spheroids may be disadvantageous for high-throughput analysis and obtaining reliable results due to low yield or uniformity issues. The droplet-based microfluidic system reported in our previous study can mass-produce uniformly sized spheroids, thereby overcoming the limitations of current spheroid production techniques [12].

In this study, we investigated the diameter of spheroids formed based on the number of encapsulated cells, and the yield of production using a droplet-based microfluidic system. This approach allows to researchers effectively produce spheroids of the desired diameters and quantity for research purposes. The benefit of producing spheroids of various diameters was leveraged to predict the optimal initiation time point and spheroid diameter for drug screening. Additionally, the morphological indicators of tumor spheroid can provide insights into the metastatic characteristics [13], as well as the surface uniformity of spheroids significantly influencing drug responsiveness [14]. Due to the importance of morphological analysis, AI, which is a powerful tool for high-throughput screening, was utilized to analyze the morphological indicators of mass-produced heterogeneous tumor spheroids. This study offers guidelines for optimizing drug screening with spheroids and potentially could contribute to the tumor drug development industry by reducing animal experiments required in early-stage drug testing [15].

2. Materials and Methods

2.1 Fabrication of device and operation

The droplet-based microfluidic system was fabricated by conventional photo and soft-lithography. PDMS replica was detached from the patterned master mold and bonded with the plasma oxygen bonding method. The droplets were generated by controlling oil and aqueous flow velocity. The aqueous phase contains tumor cells and culture media (DMEM-High glucose with 10% FBS and 1% penicillin/streptomycin, Gibco™). Oil phase contains 3M™ Novec™ 7500 engineered fluid with 5% (v/v) surfactant (FluoSurf-C™, Emulseo). Subsequently, the droplets were collected in a 35 mm petri dish and incubated in 37℃, 5% CO_2 cell incubator for 72 hours. spheroids were released using 1H,1H,2H,2H-Perfluoro-1-octanol (370533, Sigma-aldrich) to validate the diameter of the tumor spheroid. Images of spheroids in droplets were captured every 24 hours until 15 days.

2.2 Tumor cell preparation

Spheroids were fabricated from breast cancer cell lines BT474 and MCF-7. These cell lines were cultured using DMEM (Dulbecco's Modified Eagle Medium)-high glucose (11965092, Gibco™) with 10% FBS (Fetal bovine serum, 16000044, Gibco™) and 1% penicillin/streptomycin (15140122, Gibco™). When the cells 80~90% confluency, a subculture procedure was conducted. We removed the old cell culture medium and performed a single wash with 1x DPBS (Dulbecco's Phosphate-Buffered Saline, 14190144, Gibco™). Add the 0.25% trypsin-EDTA and incubate at 37℃, 5% CO_2 for 3 minutes. To prevent additional trypsin-EDTA activity, add the same volume of FBS containing growth media.

2.3 AI-tools for spheroid’s analysis

Two different artificial intelligence (AI) tools were used for performing morphological analysis of spheroids. In particular, *Analysis of Spheroids* (*AnaSP*) was used for segmenting and extracting features from 2D images

acquired using standard a brightfield widefield microscope [24]; *Reconstruction and Visualization from a Single Projection* (*ReViSP*) was used for reconstructing the 3D volume of the spheroids starting from the 2D binary masks obtained with *AnaSP*. Both *AnaSP* and *ReViSP* are open-source image processing tools developed using *MATLAB* (The MathWorks, Inc., MA, USA). *AnaSP* provides different image processing methods for tumor spheroid segmentation. They range from manual-based opportunities to fully-automated previously trained deep-learning methods [25]. When using *AnaSP*, the first step is defining the spheroid (i.e. foreground, the region of interest - ROI) and non-spheroid regions (i.e. background) based on the gray values of the image. Once the segmentations are obtained (i.e. 2D binary masks reporting in white the spheroid ROI on an artificial black background), several morphological features are automatically estimated. In particular, *AnaSP* allows the extraction of various variables, such as perimeter, area, and volume, which can then be used to calculate morphological indicators such as circularity, convexity, compactness, solidity, and sphericity. It is worth noticing that *Circularity* is a quantitative measure of how closely an object resembles a perfect circle on a 2D plane, and it is computed according to **Eq. 2**:

$$Circularity = \frac{4*\pi*Area}{ConvexPerimeter^2} \qquad \textbf{Eq. 2}$$

where *Area* is the 2D area of the spheroid's mask, and *ConvexPerimeter* is the perimeter of the convex mask. *Convexity* is a measure of how much an object deviates from being convex, and it is computed according to **Eq. 3**:

$$Convexity = \frac{ConvexPerimeter}{Perimeter} \qquad \textbf{Eq. 3}$$

where *Perimeter* is the 2D perimeter of the spheroid's mask. *Compactness* is proportional to the ratio of an object's area to its perimeter, and it is computed according to **Eq. 4**:

$$Compactness = \frac{4*\pi*Area}{Perimeter^2} \qquad \textbf{Eq. 4}$$

Solidity measures the density of an object, and it is computed according to **Eq. 5**:

$$Solidity = \frac{Area}{ConvexArea} \qquad \textbf{Eq. 5}$$

where *ConvexArea* is the 2D area of the convex mask. *Sphericity* measures the degree to which an object approaches the shape of a sphere, and it is computed according to **Eq. 6**:

$$Sphericity = \frac{\pi * EquivalentDiameter}{Perimeter} \qquad \textbf{Eq. 6}$$

where *EquivalentDiameter* is the 2D diameter of a circle having the same area as the spheroid. On the other hand, *ReViSP*, starts from a 2D binary mask created with *AnaSP* and reconstructs the 3D outer boundary of the spheroid [N01]. Practically speaking, *ReViSP* is widely used for computing the spheroid's *Volume* and obtaining the 3D shape of a spheroid using a single 2D widefield image [N02]. The method was validated using macroscopic 3D models and the only prior requirement is the general local symmetry of the spheroid and of its protuberances, which can be verified using a confocal or a light-sheet fluorescence microscope [N03].

3. Theory

3.1 Development of tumor spheroids

Tumor spheroid progression consists of three stages: cell aggregation, loose spheroid, and compact spheroid. In this developmental process, cell adhesion molecules such as integrin, cadherin proteins, and intercellular distance, play pivotal roles in spheroid formation. During the transition from cell aggregation to the loose spheroid stage, the binding of integrin to the extracellular matrix promotes spheroid formation [16]. The transition from a loose spheroid to a compact spheroid is primarily driven by the role of E-cadherin. As spheroids develop, the expression and accumulation of E-cadherin gradually increase, promoting the development of compact spheroids [17]. A compact tumor spheroid initiates the formation of a necrotic core, quiescent zone, and proliferation zone, leading to alterations in spheroid size. Tumor spheroid growth is mathematically characterized using the Gompertz model, which universally describes the initial rapid growth of spheroids as exponential growth, followed by growth plateaus caused by an increasing number of quiescent cells and the accumulation of necrotic cells inside [18]. The

growth of spheroid diameter $D(t)$ is given by **Eq. 1**:

$$D(t) = D_{max} exp\left\{-\exp(at)\ln\left(\frac{Dmax}{D_0}\right)\right\} \qquad \textbf{Eq. 1}$$

Where D_0 and D_{max} are initial and saturate tumor spheroid diameter, respectively. a is the specific growth rate and t is time. there are regions where the diameter decreases due to compaction, and in areas where proliferation dominates, the diameter of the spheroid increases. There are enhanced cellular interactions as the cell density within the spheroid increases, causing the cells to be positioned more densely, leading to compression from a spherical shape into a more compact structure [19]. Furthermore, cells located at the center of the tumor spheroid may experience further compaction in the central region due to their limited access to oxygen and nutrients compared to peripheral cells [20]. For these reasons, spheroids may not exhibit a linear increase in size depending on the culture period or the number of cells, highlighting the importance of monitoring diameter changes over time in tumor spheroids to validate reliable drug tests.

3.2 Effect on the necrotic core

The formation of necrotic cores in spheroids primarily occurs due to limited diffusion of nutrients and oxygen within the 3D structure [21]. Cells on the outer layers have relatively easy access to nutrients and oxygen from the surrounding culture medium. As the spheroid enlarges, the inner cells face challenges in obtaining these crucial resources. Nutrients and oxygen cannot efficiently penetrate deep into the spheroid due to diffusion limitations, resulting in a shortage of these essential elements for inner cells. Furthermore, without vascularization, inner cells in the spheroid are unable to receive a fresh supply of nutrients and oxygen, leading to cell death and necrosis. Therefore, predicting the diameter of spheroids where necrotic cores form is important because overlapping of cell death induced by the necrotic core and drug effects can lead to bias in drug response evaluation.

4. Result and Discussion

4.1 Production of spheroids

Droplet-based microfluidic systems can overcome the limitations associated with several methods for spheroid production, as described in Table 1, such as throughput, labor intensity, and uniformity. Figure 1(a) shows the production process of tumor spheroids using a droplet-based microfluidics system. Figure 1(b) shows that this system fabricated droplets with diameters of 0.5mm, 1.1mm, and 1.4mm at rates of 21Hz, 2.15Hz, and 0.85Hz, respectively. We calculated the spheroid diameter based on the number of encapsulated cells per droplet, as shown in Figure 1(c). This result shows that spheroid diameter increases non-linearly depending on the number of cells encapsulated in the droplet. To fabricate spheroids of 300μm, approximately 7.01 times more cells are needed compared to 150μm. Figure 1(d) shows the diameter distribution of spheroids with intended diameters of 100μm, 250μm, and 450μm. Approximately 41%, 61%, and 85% of the spheroids were distributed within a range of ±10% of their intended diameters for 100μm, 250μm, and 450μm, respectively. This finding indicates that as the diameter of a spheroid increases, it becomes more advantageous for producing spheroids with the intended diameter. This is because larger spheroids are less affected by variations in cell concentration, as shown in Figure 1(d). Furthermore, utilization of large spheroids can give benefits for reliable results of drug screening, because large spheroids (with a diameter >500μm) can mimic various characteristics of human solid tumors with sizes ranging from 0.5 to 1 mm^3, offering the potential for more accurate drug response validation [22].

Table 1. Comparison of spheroid fabrication methods

Hanging drop plate	**Micro-cavity method**	**Low-attachment plate**	**Droplet-based microfluidics**
Low throughput	Low throughput	High throughput	High throughput
Labor intensity	Labor intensity	Easy to use	Automated fabrication
Uniform size	Uniform size	Non-uniform size	Uniform size

4.2 Spheroid diameter and culture period

Figure 2(a) shows that tumor spheroids do not proliferate a linear growth trend. Compaction is a unique phenomenon observed during the formation of spheroids, which is not typically found in monolayer cultures [23]. BT474 spheroid with diameters of >400μm and <400μm were produced and their diameter changes were observed, as shown in Figure 2(b). Figure 2(c) shows the change in diameter of spheroids with a diameter of <400μm. The diameter decreased during the early stages of culture (~ day 3), followed by an increase (day 3~7). Then, the diameter remained relatively constant for 4 days (day 7~10), and there was a secondary increase (~ day 15). For spheroids with a diameter >400μm, the diameter decreased (~day 4), then increased (day 4~9). Subsequently, the diameter remained relatively constant for 4 days (day 9~12), and the secondary increase was not observed, as shown in Figure 2(d). Spheroids with diameters of >400μm and <400μm increased by 19% and 8%, respectively, from the initial day to day 15.

The diameter decreased during the compaction phase (~ day 3 or 4) when compact tumor spheroids were formed. Moreover, there was a tendency to agree with the Gompertz model, which describes subsequent rapid growth and a growth plateau after the compact phase. These results provide significant criteria in the validation of drug screening based on spheroid diameters for assessing the effects of drugs. When tumor spheroids are exposed to drugs during the compaction phase, the presence of variables related to self-compaction may lead to bias in accurately analyzing the remission effect. Applying the drug during the increase phase, following the compaction phase, guarantees a more accurate evaluation of the drug effect. Spheroids with diameters of <400μm and >400μm should be cultured for a minimum of 3 days and 4 days, respectively, to assess the effectiveness of the drug test.

4.3 Analysis of the necrotic core formation

We investigated the formation of a necrotic core based on the diameter of the spheroids. Figure 3(a) shows the formation of a necrotic core at the center of the spheroid as its size increases. Figure 3(b) is a microscopic

fluorescent image of the spheroid, showing the presence of a necrotic core (blue: nucleus, red: dead cells). To determine the spheroid diameter at which the necrotic core forms, the number of viable cells was measured as a function of the spheroid diameter, as shown in Figure 3(c). Among the spheroids cultured for 4 days, the number of live cells in small spheroids within the diameter range of 73.4μm to 148.3μm was observed to increase exponentially as the diameter increased. On the other hand, at the larger spheroid diameters of 328μm and 371μm, 3,389 and 2,321 live cells were detected, indicating a decreasing trend. This result suggests that when spheroids reach a specific size, spheroids begin to undergo the formation of a necrotic core. We predicted that necrotic core formation would occur at the diameter (315.3μm) where the cell growth trendline (black dashed line) intersects with the cell decline trendline (red dashed line) in Figure 3(c). As mentioned above, a large spheroid (with a diameter >500μm) offers the potential for more accurate validation of drug responses. However, when both necrotic core formation and drug-induced cell death occur simultaneously, it becomes challenging to accurately assess drug responses. Consequently, to mitigate the impact of a necrotic core, a spheroid with a maximum diameter of 315.3μm can be regarded as the ideal size for drug screening.

4.4 Morphological analysis of spheroids

Morphological analysis is crucial for conducting high-throughput screening verification, especially when working with various groups of spheroids that exhibit differences in sizes, volumes, and extracted parameters [26]. In particular, morphological analysis is frequently employed for assessing drug responsiveness in tumor spheroids due to its ability to provide quantitative, high-throughput, and non-invasive profiling [27, 28]. Therefore, we performed morphological analysis of mass-produced spheroids using *AnaSP* and *ReViSP*. Figure 4(c) shows the 3D reconstructions obtained with *ReViSP* from the 2D spheroid's segmentations created by an expert operator using the manual opportunities provided by *AnaSP*. Figure 4(d) shows the spheroid parameters extracted from Figure 4(a), portraying the surface characteristics of MCF-7 spheroids (average diameter: 183.73±11.92μm,

average volume: 2.96±0.54nL). Figure 5(a, b) shows heterologous breast tumor spheroids of BT474 and MCF-7 with diameters of 100, 200, and 300μm for 3 days culture period, and AI-based comparative analysis of the morphological indicators (circularity, convexity, and compactness) was conducted, as shown in Figure 5(c, d). Figures 5(a, c) show BT474 spheroids within droplets for 3 days. For BT474 spheroids, an increasing trend in all morphological indicators was observed. This result indicates that BT474 spheroids can maintain an independent environment within the droplet for 3 days and preserve their 3D structure. On the other hand, MCF-7 spheroids with diameters of 100 and 200μm for 3 days increased morphological indicators for the first 2 days, followed by a decreasing trend. MCF-7 spheroids with a diameter of 300μm consistently exhibited decreased morphological indicators for 3 days. This difference is likely due to the different metabolic rates of BT474 and MCF-7. The doubling times for BT474 and MCF-7 are approximately 38 hours and 24 hours, respectively, and as the proliferation rate increases, cells need to synthesize more internal content, which is positively correlated with metabolic rate [29]. This result suggests that the optimal culture conditions of spheroids for morphological analysis may vary depending on the cell type and its metabolic characteristics, emphasizing the importance of controlling the morphological features of spheroids (e.g. diameter and sphericity) and culture periods for specific experimental purposes.

5. Conclusion

We provided guidelines for the mass production of uniform tumor spheroids and investigated compaction, diameter changes, and necrotic core formation based on spheroid diameter for the optimal conditions of drug efficacy assessments. It is advisable to culture spheroids with diameters of <400μm and less for 3 days to ensure compaction has occurred before conducting drug efficacy testing, and for spheroids >400μm, a 4-day culture period is recommended to adequately validate drug efficacy. Moreover, it is important to optimize spheroid diameter while considering the presence of necrotic cores before performing drug screening and viability

measurements. We predicted the formation of a necrotic core in spheroids at a diameter of approximately 315.3μm, which represents the optimal diameter for drug screening to mitigate potential analysis bias. We also emphasized the importance of AI program-based morphological analysis to enable precise and high-throughput screening for the analysis of mass-produced spheroids. Morphological indicators such as circularity, convexity, and compactness were measured through AI-based analysis. Depending on the diameter of spheroids, the culture period, and cell types, different morphological indicators were observed. Recently, in addition to the growing interest in tumor spheroids, this study provided an optimized conditions for effective drug screening and presented an AI-based morphological analysis method for high-speed screening.

Acknowledgments

This study was supported by the National Research Foundation of Korea (NRF) grant funded by the Korean government (MEST) (NRF-2022R1A2C2003103). F.P., and G.C. acknowledge support from the MAECI Science and Technology Cooperation Italy-South Korea Grant Years 2023–2025 by the Italian Ministry of Foreign Affairs and International Cooperation (CUP project: J53C23000300003).

Declarations

Conflict of Interest The authors declare that they have no conflict of interest.

References

1. IMAMURA, Y. et al. Comparison of 2D- and 3D-culture models as drug-testing platforms in breast cancer. Oncology Reports 33, 1837–1843 (2015).

2. Kapałczyńska, M. et al. 2D and 3D cell cultures – a comparison of different types of cancer cell cultures. Archives of Medical Science (2016).

3. Choi, N. Y., Lee, M.-Y. & Jeong, S. Recent advances in 3D-cultured brain tissue models derived from human ipscs. BioChip Journal 16, 246–254 (2022).

4. Ravi, M., Paramesh, V., Kaviya, S. R., Anuradha, E. & Solomon, F. D. P. 3D cell culture systems: Advantages and applications. Journal of Cellular Physiology 230, 16–26 (2014).

5. Białkowska, K., Komorowski, P., Bryszewska, M. & Miłowska, K. Spheroids as a type of three-dimensional cell cultures—examples of methods of preparation and the most important application. International Journal of Molecular Sciences 21, 6225 (2020).

6. Kimlin, L. C., Casagrande, G. & Virador, V. M. In vitro three-dimensional (3D) models in cancer research: An update. Molecular Carcinogenesis 52, 167–182 (2011).

7. Yeon, J. H., Chung, S. H., Baek, C., Hwang, H. & Min, J. A simple pipetting-based method for encapsulating live cells into multi-layered hydrogel droplets. BioChip Journal 12, 184–192 (2018).

8. Kang, S.-M. Recent advances in microfluidic-based microphysiological systems. BioChip Journal 16, 13–26 (2021).

9. Foty, R. A simple hanging drop cell culture protocol for generation of 3D spheroids. Journal of Visualized Experiments (2011). doi:10.3791/2720-v

10. Kloß, D., Fischer, M., Rothermel, A., Simon, J. C. & Robitzki, A. A. Drug testing on 3D in vitro tissues trapped on a microcavity chip. Lab on a Chip 8, 879 (2008).

11. Kochanek, S. J., Close, D. A. & Johnston, P. A. High content screening characterization of head and neck squamous cell carcinoma multicellular tumor spheroid cultures generated in 384-well ultra-low attachment plates to screen for better cancer drug leads. ASSAY and Drug Development Technologies 17, 17–36 (2019).

12. Kwak, B., Lee, Y., Lee, J., Lee, S. & Lim, J. Mass fabrication of uniform sized 3D tumor spheroid using high-throughput microfluidic system. Journal of Controlled Release 275, 201–207 (2018).

13. Moriconi, C. et al. INSIDIA: A Fiji macro delivering high-throughput and high-content spheroid invasion analysis. Biotechnology Journal 12, (2017).

14. Zanoni, M. et al. 3D tumor spheroid models for in vitro therapeutic screening: A systematic approach to enhance the biological relevance of data obtained. Scientific Reports 6, (2016).

15. Bédard, P. et al. Innovative human three-dimensional tissue-engineered models as an alternative to animal testing. Bioengineering 7, 115 (2020).

N01. Piccinini, F., Tesei, A., Arienti, C., & Bevilacqua, A. Cancer multicellular spheroids: volume assessment from a single 2D projection. Computer Methods and Programs in Biomedicine, 118(2), 95-106 (2015).

N02. Mishra, A., Kai, R., Atkuru, S., Dai, Y., Piccinini, F., Preshaw, P. M., & Sriram, G. Fluid flow-induced modulation of viability and osteodifferentiation of periodontal ligament stem cell spheroids-on-chip. Biomaterials Science, 11(22), 7432-7444 (2023).

N03. Diosdi, A., Hirling, D., Kovacs, M., Toth, T., Harmati, M., Koos, K., Buzas, K., Piccinini, F. & Horvath, P. Cell lines and clearing approaches: a single-cell level 3D light-sheet fluorescence microscopy dataset of multicellular spheroids. Data in Brief, 36, 107090 (2021).

16. Lin, R. & Chang, H. Recent advances in three-dimensional multicellular spheroid culture for biomedical research. Biotechnology Journal 3, 1285–1285 (2008).

17. Lin, R.-Z., Chou, L.-F., Chien, C.-C. M. & Chang, H.-Y. Dynamic analysis of Hepatoma spheroid formation: Roles of E-cadherin and β1-integrin. Cell and Tissue Research 324, 411–422 (2006).

18. Koike, C. et al. Solid stress facilitates spheroid formation: Potential involvement of hyaluronan. British Journal of Cancer 86, 947–953 (2002).

19. Pinto, B., Henriques, A. C., Silva, P. M. & Bousbaa, H. Three-dimensional spheroids as in vitro preclinical models for cancer research. Pharmaceutics 12, 1186 (2020).

20. Nath, S. & Devi, G. R. Three-dimensional culture systems in cancer research: Focus on tumor spheroid model. Pharmacology & Therapeutics 163, 94–108 (2016).

21. Park, S. Y., Hong, H. J. & Lee, H. J. Fabrication of cell spheroids for 3D cell culture and biomedical applications. BioChip Journal 17, 24–43 (2022).

22. Nath, S. Devi, G. R. Three-dimensional culture systems in cancer research: Focus on tumor spheroid model. Pharmacology & Therapeutics 163, 94–108 (2016).

23. Ferrante, A., Rainaldi, G., Indovina, P., Indovina, P. & Santini, M. Increased cell compaction can augment the resistance of HT-29 human colon adenocarcinoma spheroids to ionizing radiation. International Journal of Oncology (2006). doi:10.3892/ijo.28.1.111

24. Piccinini, F. AnaSP: A software suite for automatic image analysis of multicellular spheroids. Computer Methods and Programs in Biomedicine 119, 43–52 (2015).

25. Piccinini, F., Peirsman, A., Stellato, M., Pyun, J.C., Tumedei, M.M., Tazzari, M., De Wever, O., Tesei, A., Martinelli, G. & Castellani, G. Deep Learning-Based Tool for Morphotypic Analysis of 3D Multicellular Spheroids. Journal of Mechanics in Medicine and Biology, 23(6), 2340034 (2023).

26. Kim, C. Droplet-based microfluidics for making uniform-sized cellular spheroids in alginate beads with the regulation of encapsulated cell number. BioChip Journal 9, 105–113 (2015).

27. Aguilar Cosme, J. R., Gagui, D. C., Bryant, H. E. Claeyssens, F. Morphological response in cancer spheroids

for screening photodynamic therapy parameters. Frontiers in Molecular Biosciences 8, (2021).

28. Shirai, K. et al. The importance of scoring recognition fitness in spheroid morphological analysis for robust label-free quality evaluation. Regenerative Therapy 14, 205–214 (2020).

29. Zhu, J. & Thompson, C. B. Metabolic regulation of cell growth and proliferation. Nature Reviews Molecular Cell Biology 20, 436–450 (2019).

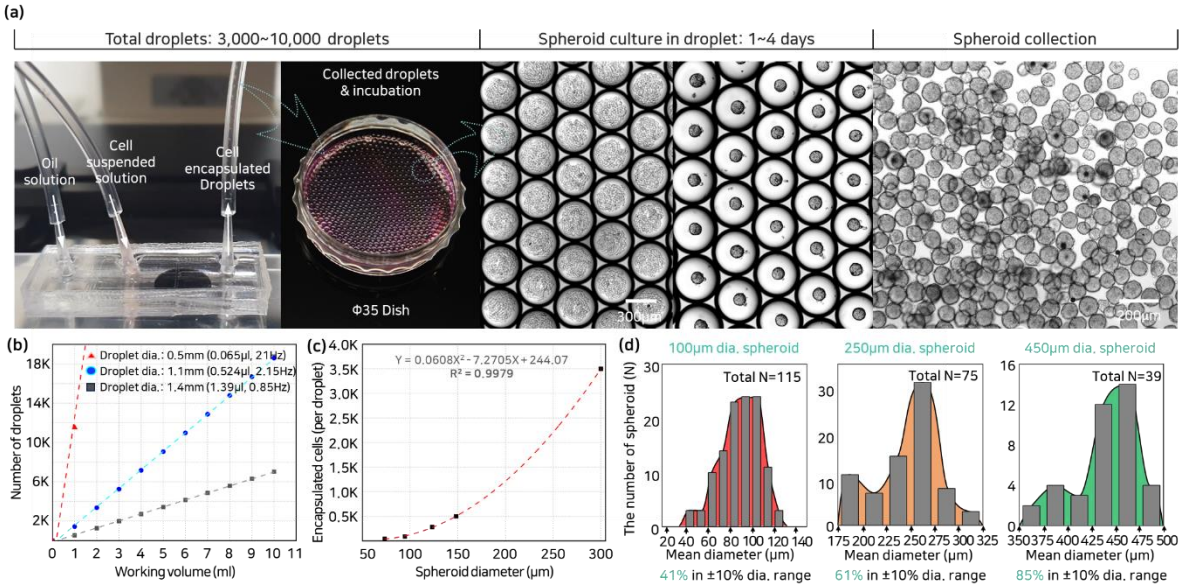

Figure 1. (a) Process of tumor spheroid mass production using droplet based microfluidic system. (b) the required media volume and production yield for producing droplets with diameters of 0.5, 1.1, and 1.4 mm. (c) the correlation between the tumor spheroid diameter and the number of cells encapsulated within droplets. (d) size distribution of intended 100, 250, and 450μm diameters of tumor spheroids.

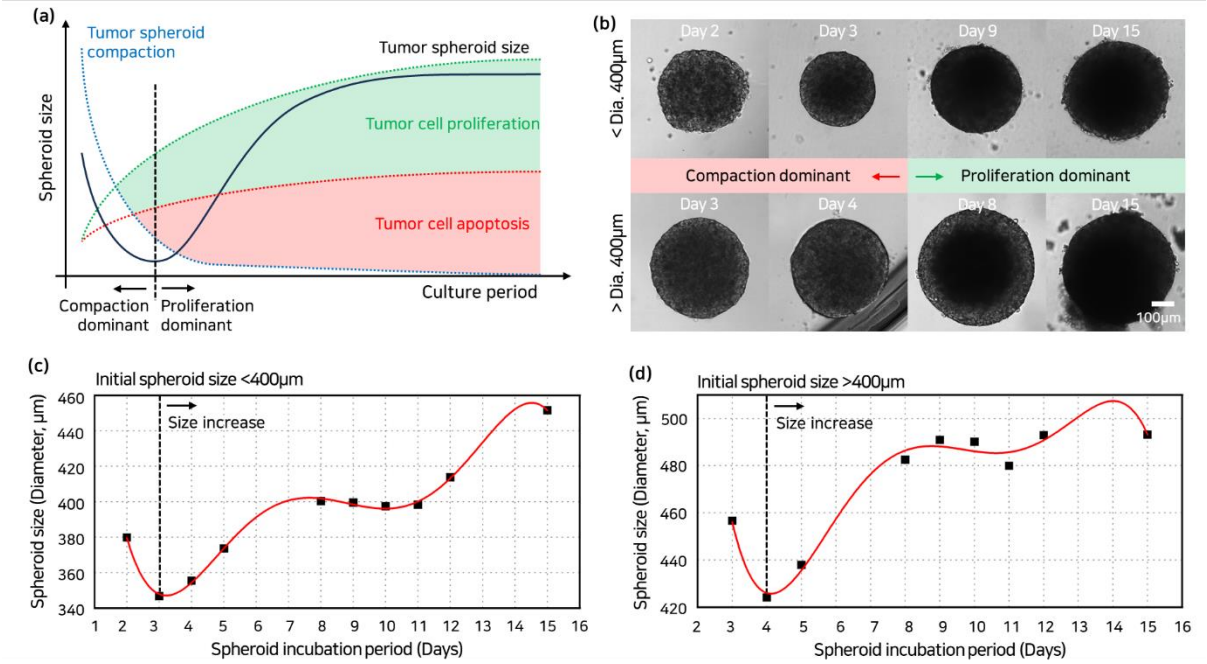

Figure 2. (a) Schematic diagram of correlation between the culture period and the change in tumor spheroid size. (b) microscopic images of comparing compaction and proliferation periods based on BT474 tumor spheroid size. (c, d) graph of changes in the diameter of tumor spheroids based on the culture period for sizes >400μm and <400μm.

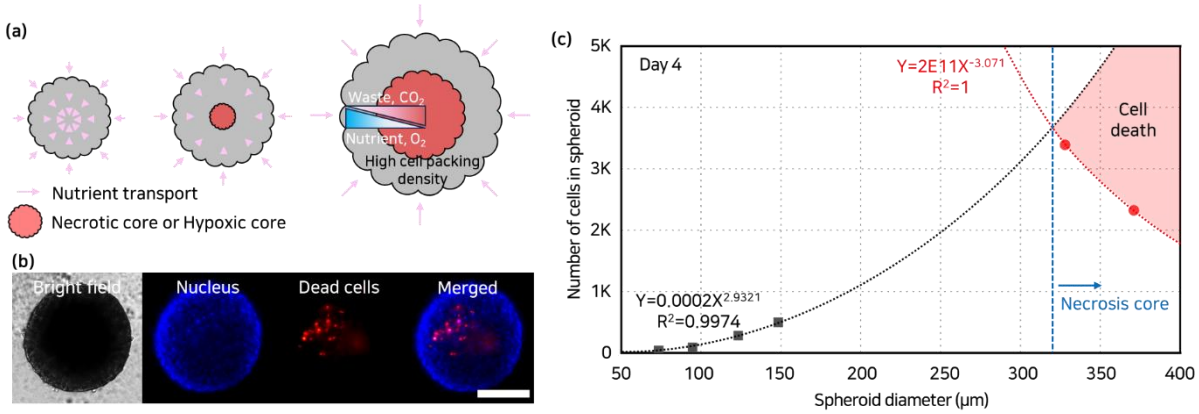

Figure 3. (a) Schematic image of necrotic core formation under the size increment conditions. (b) nucleus and dead cell fluorescent images of BT474 tumor spheroid (scale bar: 200μm). (c) a predictive graph of necrosis core formation based on the number of live cells encapsulated in tumor spheroids.

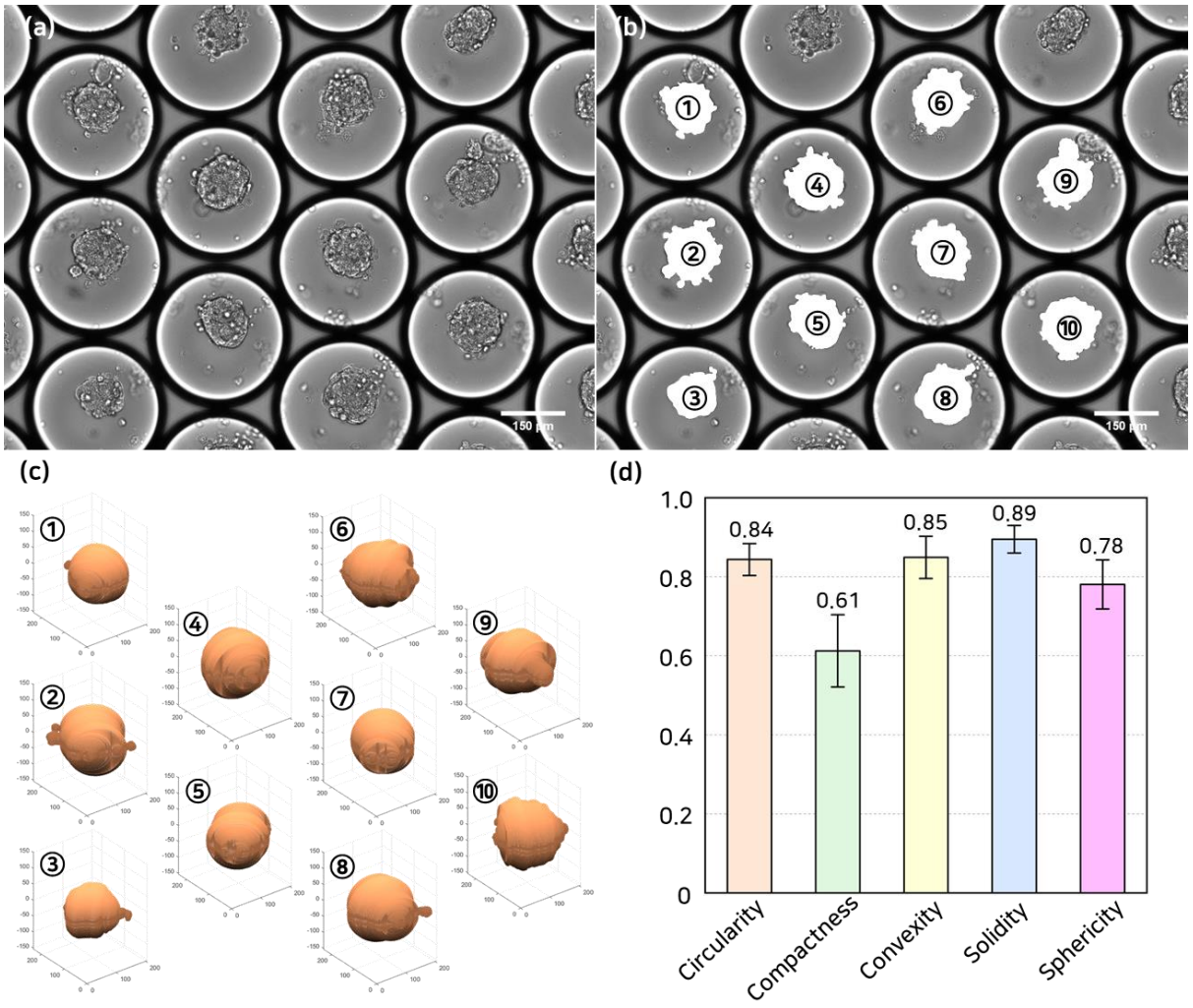

Figure 4. (a) Microscopic brightfield images of tumor spheroids encapsulated in droplets. (b) Segmentations obtained analyzing the captured spheroid images with *AnaSP*. (c) 3D rendering of tumor spheroids automatically created with *ReViSP* starting from the segmentations of the microscopic images. (d) Morphological indicators of tumor spheroids extracted using AI-based algorithms.

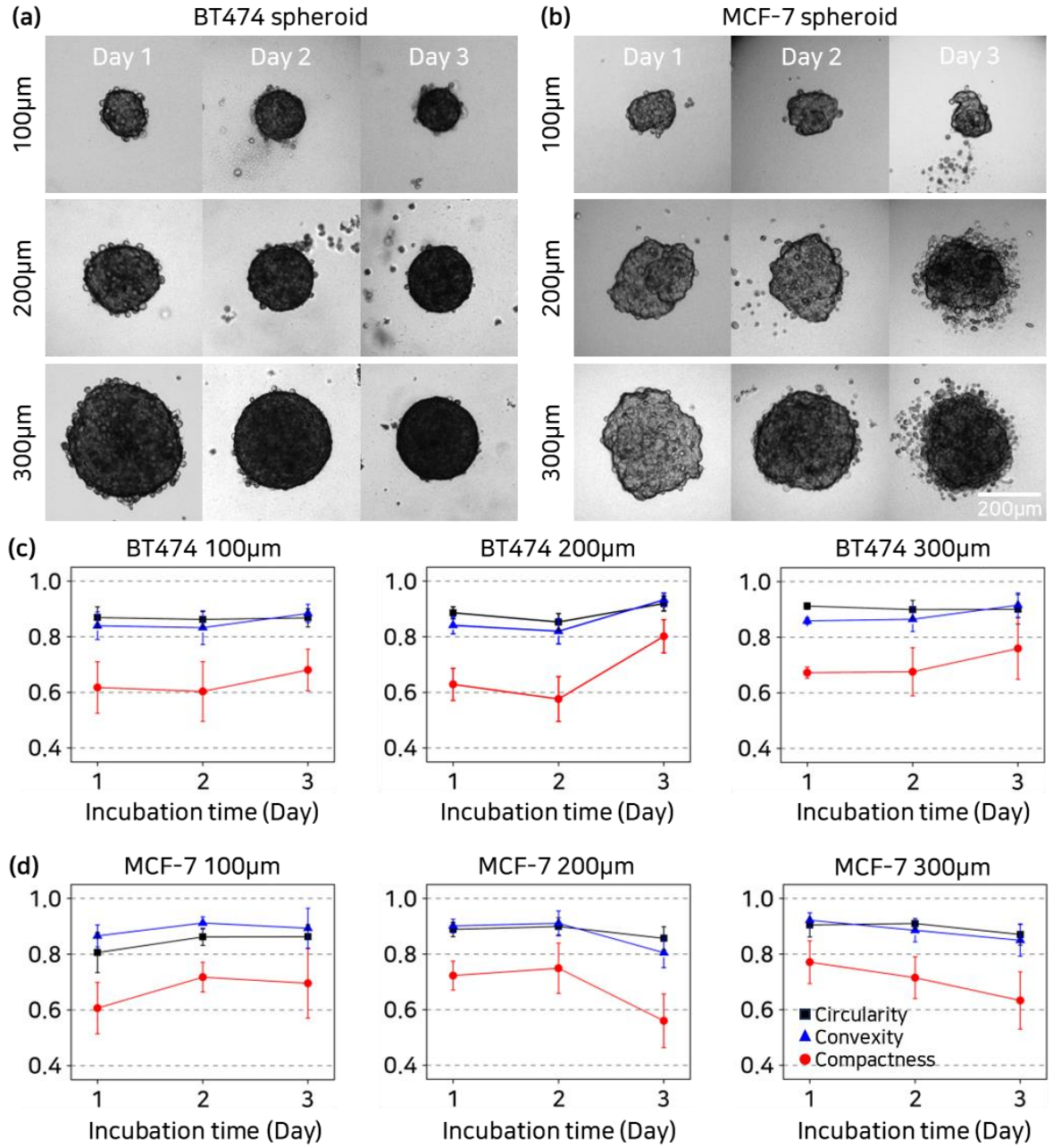

Figure 5. (a, b) The morphological changes of culturing 100, 200, and 300μm BT474 and MCF-7 tumor spheroids within droplets for 3 days. (c, d) morphological indicator (circularity, convexity, and compactness) changes of culturing 100, 200, and 300μm BT474 and MCF-7 tumor spheroids within droplets for 3 days.